ACS OMEGA

Article

Cite This: ACS Omega 2019, 4, 6726−6736

http://pubs.acs.org/journal/acsodf

Identification of Specific Lysines and Arginines That Mediate Angiomotin Membrane Association

Le'Celia Hall,[†,‡] Emily Donovan,[†,§] Michael Araya,[†,∥] Eniola Idowa,[†,⊥] Ilse Jiminez-Segovia,[†] Anthony Folck,[†,#] Clark D. Wells,[†] and Ann C. Kimble-Hill*[,†]

[†]Department of Biochemistry and Molecular Biology, Indiana University School of Medicine, Room MS 4053, 635 Barnhill Drive, Indianapolis, Indiana 46202, United States

ABSTRACT: The family of Angiomotin (Amot) proteins regulate several biological pathways associated with cellular differentiation, proliferation, and migration. These adaptor proteins target proteins to the apical membrane, actin fibers, or the nucleus. A major function of the Amot coiled-coil homology (ACCH) domain is to initiate protein interactions with the cellular membrane, particularly those containing phosphatidylinositol lipids. The work presented in this article uses several ACCH domain lysine/arginine mutants to probe the relative importance of individual residues for lipid binding. This identified four lysine and three arginine residues that mediate full lipid binding. Based on these findings, three of these residues were mutated to glutamates in the Angiomotin 80 kDa splice form and were incorporated into human mammary cell lines. Results show that mutating three of these residues in the context of full-length Angiomotin reduced the residence of the protein at the apical membrane. These findings provide new insight into how the ACCH domain mediates lipid binding to enable Amot proteins to control epithelial cell growth.

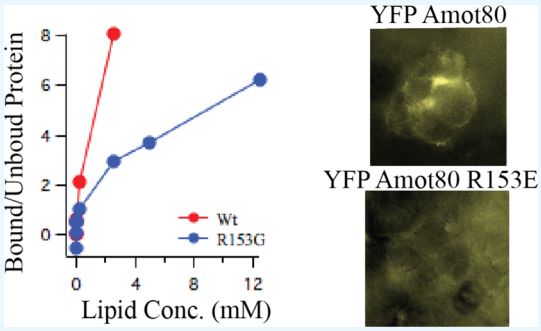

INTRODUCTION

The family of Angiomotin (Amot) proteins regulate several biological pathways associated with cellular differentiation, proliferation, and migration. The Amot adaptor protein integrates the control of cellular morphology with its proclivity to proliferate.[1−3] This is mainly accomplished through the differential ability of specific isoforms of Amot to orient the trafficking of proteins that regulate apical cell polarity with proteins involved in the HIPPO growth control pathway.[1,4] Amot localization is determined by membrane association, an essential and conserved feature controlled by its lipid affinity comprised of the novel Amot coiled-coil homology (ACCH) domain.[5] This domain, while sharing some features of BAR domains, specifically predicts a coiled-coil fold of approximately 240 residues. This differs from classical BAR domains in that it has the unique property of being able to selectively bind phosphatidylinositols (PIs) and cholesterol.[5] However, the mechanism by which the ACCH domain screens for these lipids is currently unknown.

To address this gap in knowledge, we investigated the mechanisms used by three classic domains that target PIs. The FYVE domain contains a positively charged pocket that has selective affinity for monophosphorylated PI based on exclusion criteria predicated on the size of the headgroup.[6,7] The plekstrin homology (PH) domain contains a basic pocket with a loop rich in lysines, arginines, and hydrophobic amino acids that provides a size specificity towards di- and triphosphorylated PIs.[6,8] Finally, the Phox consensus sequence (PX) motif specifically binds monophosphorylated PI3P via a basic binding pocket.[6] Similar to these domains, the ACCH domain is also rich in lysines and arginines. Therefore, we hypothesized that the enrichment of these positively charged residues in the ACCH domain is essential for targeting Amot to PI-containing membranes.

This report details the determination of specific arginine and lysine residues within the ACCH domain that mediate the overall affinity for PI. To that end, site-directed mutagenesis was employed to probe the specific contributions of each lysine and arginine residue by changing them to nonpositively charged amino acids and evaluating the resulting ability to associate to specific PI-containing membranes by lipid sedimentation and native tyrosine fluorescence quenching. From those screens, eight lysines and arginine residues were selected and characterized for changes in binding affinity. Finally, in vitro experiments confirmed that three of these residues, whose mutation in the context of Amot80 led to a change in its cellular localization, are required for full membrane binding.

RESULTS

Fluorescence Quenching. The binding affinity of the ACCH domain for specific lipid compositions was measured by the degree of tyrosine residue fluorescence quenching as a function of the concentration of various dansylated liposomes.

Received: January 17, 2019
Accepted: March 28, 2019
Published: April 12, 2019

DOI: 10.1021/acsomega.9b00165
ACS Omega 2019, 4, 6726−6736

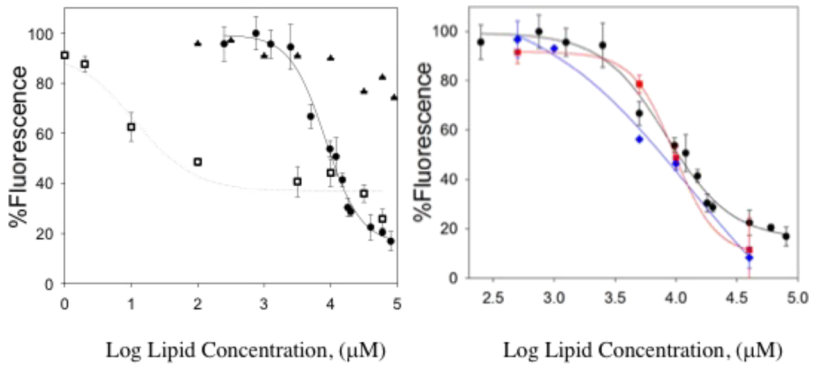

ACCH Domain	AC50 (mM)	Std Error	R^2
Amot80	11.5	0.001	0.8968
AmotL1	9.66	0.001	0.9621
AmotL2	13.0	0.003	0.985

Figure 1. Quenching of Amot80 ACCH domain tyrosines by POPC (solid triangle), 3/1/1 molar ratio POPC/POPE/PI (black circle), and 2/1/1/1 molar ratio POPC/POPE/PI/Chol (box) liposomes that included 5 mol % dansyl DHPE. Additionally, measurements from AmotL1 (red box) and AmotL2 (blue diamond) ACCH domain tyrosine quenched by dansylated POPC/POPE/PI are provided. Error bars are the standard deviation of $n = 3$ measurements. The fits of these measurements are also reported as AC50, with the respective standard error and R^2 values for the fit.

In general, increasing the amount of PI-containing lipid resulted in a decrease in tyrosine fluorescence. This indicates that the liposomes were coming into close proximity to and quenched the fluorescence of the ACCH domain tyrosines (Figure 1). Furthermore, the AmotL1 and AmotL2 ACCH domains bound liposomes with a similar affinity as Amot80, with around 50% of the protein bound at 8.32 mM POPC/POPE/PI (3/1/1) liposomes, whereas no significant binding for any ACCH domain was seen for POPC liposomes. Similar to results previously reported using surface plasmon resonance,[5] a 10-fold higher affinity of the ACCH domain for liposomes containing 20 mol % cholesterol was observed. Fluorescence quenching data also indicated a first-order correlation between total lipid concentration and protein bound. Hence, all screening assays for detecting decreasing lipid affinity were carried out at a saturating concentration of 20 mM lipid.

Mutant Library Screen. Based on the hypothesis that positively charged residues in the ACCH domain mediate binding to PIs similar to BAR, PH, and PX, and FYVE domains, we used the WebLogo tool to determine the charge conservation of the residues between the ACCH domains of Amot80, AmotL1, and AmotL2, with a particular interest in the positively charged arginines and lysines. The resulting alignments guided our choice of residues to query further by site-directed mutagenesis (Figure 3). A basic charge or an exposed amine group based on pH was conserved for all lysine and arginine residues except Lys126, Arg153, and Lys185.

Lys126 corresponds to an alanine and aspartate in AmotL1 and AmotL2, respectively. A BLAST search among all known and predicted AmotL1 across species shows that this alanine is completely conserved, as is the aspartate in AmotL2. We therefore mutated this residue to a glutamate to give Amot a similar charge−charge interaction as AmotL2.

Lys185 is conserved in AmotL2 but is a glutamate in AmotL1. In this study, we mutated Lys185 to the same interactions of AmotL1 while maintaining a similar space of the other two family members.

Arg153 is conserved as an arginine in AmotL1, but using the Weblogo alignment, we found that this residue is a highly conserved, hydrophobic, slightly smaller leucine next to the arginine in AmotL2. Therefore, mutating Arg153 into a glutamate in this study reversed the charge while occupying the same space as all of the Amot family members. A glycine mutant was also constructed for our screening studies, which is a much smaller, noncharged residue than either residue seen naturally.

The lack of a significant difference in the AC50 values between family members suggests that a similar membrane association would be observed when Lys126 and Lys185, and not Arg153, were mutated to encode a negatively charged residue.

Charge conservation was further observed for lysine residues at positions 49, 52, 55, 62, 72, 82, 85, 87, 94, 103, 105, 111, 142, 144, 166, 179, 193, 196, 210, 217, 219, and 234. Such conservation suggests that these residues participate in membrane association. Site-directed mutagenesis was carried out at the majority of these residues to encode a glutamate to reverse the charge while retaining a similar occupying space as the original acidic residue. Additional mutations that encode a serine or threonine result in an exposed negatively charged nucleophile at the original positively charged amine group. When neither of these mutation classes proved possible, the residue was mutated to a glycine. All of these mutations are described in Figure 3. Based on our hypothesis, we expected to see the most significant reduction in membrane association for mutations where the residue charge was the most conserved.

To screen mutants for decreased lipid binding, we first used the fluorescence quenching assay. In this assay, each mutant was screened for tyrosine fluorescence before and after lipid binding at a singular lipid concentration and compared to the results obtained with the wild-type protein. Relative fluorescence after lipid association was calculated using eq 1, and the percent change in fluorescence with respect to the wild-type protein was calculated for each mutation (Figure 3). Of the residues tested, Arg52, Lys82, Arg85, Lys87, Arg105,

DOI: 10.1021/acsomega.9b00165
ACS Omega 2019, 4, 6726−6736

Arg153, Arg166, Lys179, Lys187, Lys193, Arg219, and Arg234 resulted in greater than 40% reduction in lipid binding.

Differences in lipid binding for each mutant was validated by measuring their sedimentation with liposomes (Figure 2).

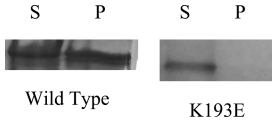

Figure 2. Representative sedimentation gels for Amot and various mutants incubated with POPC/POPE/PI (3/1/1 mole fraction). The left lane was from the supernatant (S), and the right lane was collected from the lipid pellet fraction (P).

While sedimentation assays are generally more of a qualitative tool for measuring relative affinity, the advantage of this assay is its independence from the requirement that the protein be in close proximity to the dansylated lipid headgroup that could be sequestered to PI-driven phase separations, which is then later reorganized by the ACCH domain.[9] Therefore, we did an initial screen of the change in the ratio of protein bound/unbound relative to the wild-type protein and reported it as percent change (Figure 3). In these experiments, mutations at residues Arg24, Lys49, Arg52, Lys82, Arg85, Lys87, Arg103, Arg153, Arg166, Lys179, Lys193, Lys210, and Arg219 resulted in a 40% or greater reduction in lipid binding relative to the wild-type protein.

While mutations in nonconserved residues including Arg24, Lys116, Lys126, Lys134, Lys136, Lys185, and Arg224 have little to no effect on lipid binding, the Arg153 mutant had a significant decrease in association to membranes, whereas mutations in eight conserved positively charged residues resulted in a significant loss of membrane binding.

In summary, mutations in nine residues (Arg52, Lys82, Arg85, Lys87, Arg153, Arg166, Lys179, Lys193, and Arg219) resulted in at least a two-fold decrease in binding by both screens (Figure 3). All of these mutants also showed reduced binding by triplicate measurements of fluorescence quenching (Figure 4). Each of these mutations were further characterized by their effect on nonrelated functions, such as ability to oligomerize, and the lipid binding AC50.

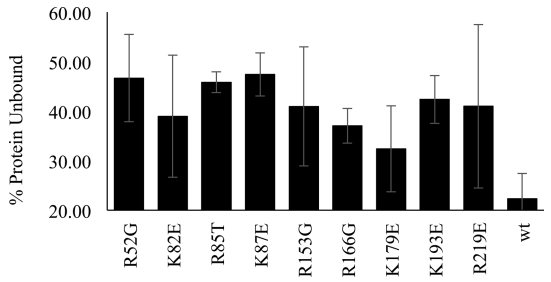

Figure 4. Verification of mutations from an initial screen. Mutations that initially showed at least a 40% reduction in association (Figure 3) were verified in triplicate using the fluorescence quenching assay. All mutations led to approximately a 2-fold reduction in membrane-associated protein.

Mutation Effect on Native Protein Function. The ACCH domains of Amot family members also oligomerize, a key function that is implicated in their roles in cells.[10−13] This study was designed to exclude mutations that had significant affects beyond membrane association, such as a loss of globular structural features. Each mutant was therefore also characterized for differences in oligomerization using size exclusion chromatography. Only the Arg85 mutant showed a loss of higher-order molecular weights (Figure 5). All other mutants therefore appear to form homo-oligomers in a similar fashion as the wild-type domain. As a result, R85T was excluded from further analysis.

Characterization of Mutant-Lipid Binding Affinity. The fluorescence quenching assay was employed to measure the lipid binding AC50 for each of the resulting mutants to identify residues that participate in lipid binding (Table 2). Mutation of a residue that participates in lipid binding should lead to an increase in the AC50 for the fluorescence quenching. Here, we found that mutating Lys82 and Arg219 did not have a significant effect on lipid binding. Mutating Arg153 and

Figure 3. Changes in ACCH domain liposome binding based on residue mutations. A WebLogo (http://weblogo.berkeley.edu) representation of the negatively charged residues in the Amot80/130 ACCH domain studied in our library shows the residue and charge conservation with the AmotL1 and AmotL2 ACCH domain sequences. Lipid binding to each mutant was initially screened by the sedimentation and fluorescence quenching assay where mutations are shaded based on changes in binding: ≥40% increase (red box), ≥20% increase (pink box), ≥20% reduction (gray box), and ≥40% reduction (black box).

DOI: 10.1021/acsomega.9b00165
ACS Omega 2019, 4, 6726−6736

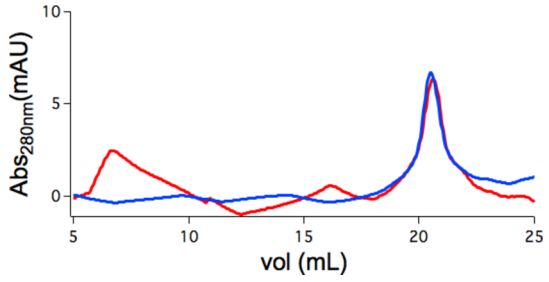

Figure 5. Oligomeric states of the ACCH domain in solution. Size exclusion chromatography elution profile of purified wild type (red line) showing three peaks corresponding to a monomer of ~36 kDa (~21 mL), a tetramer of ~135 kDa (~16 mL), and a large aggregate (~8 mL). The chromatograph of the R85T mutant (blue line) shows a peak that corresponds to the monomer and unappreciable amounts of oligomers.

Table 1. Summary of Lipid-Related AC50 for Wild-Type Protein (n = 3)[a]

lipid composition	AC50 (mM)	std error
POPC	NB	NB
POPC/POPE/soy PI(3/1/1)	11.5	0.001
POPC/POPE/soy PI/Chol(2/1/1/1)	0.014	0.001

[a]NB = no binding activity.

Table 2. Lipid Binding Affinities for POPC/POPE/soy PI (3/1/1) Vesicles Determined by Fluorescence Quenching (n = 3)

mutation	AC50 (mM)	std error	fold change
R52G	125	0.004	4
K82E	28.2	0.001	1
K87E	63.1	0.003	2
R153G	39.8	0.003	1
R166G	48.4	0.002	2
K179E	63.1	0.003	2
K193E	50.1	0.003	2
R219E	25.1	0.002	1

Lys193 led to only moderate increases in AC50 values. In contrast, mutating Arg52, Lys87, and Lys179 caused at least a two-fold increase in the AC50 value.

The protein lipid overlay (PLO) assay was then employed to further study the effect of these mutations on the lipid binding affinity (Table 3). Unlike the fluorescence quenching assay that utilizes multilayer lamellar vesicles with fluorescently labeled lipid headgroups incorporated throughout the entire mixture, the PLO assay requires the lipid to be adsorbed on the surface of a nitrocellulose membrane providing a single layer for protein interaction. As the nitrocellulose is a stationary phase for presentation of the lipid, the protein is only able to associate with the presented lipid and cannot perform the lipid phase reorganization or membrane fusion activities of the domain that is seen in the other experimental assays used in this study. Furthermore, we utilized the POPC/POPE/PI/Chol (2/1/1/1 molar ratio) lipid mixture that was previously reported to have a four-fold higher affinity for the ACCH domain using surface plasmon resonance versus the POPC/POPE/PI (3/1/1 molar ratio) liposomes used in the fluorescence quenching assay.[5] Both of these effects led to an ~1000× lower reported AC50 value for the PLO assay than previously described (Figure 1A and Tables 1 and 3). Figure 6 shows a representative blot from this experiment. In this assay, we found that mutating Lys87 and Arg219 had no significant effect on their binding affinity for POPC/POPE/soy PI/Chol (2/1/1/1 molar ratio)-containing liposomes. This confirms results seen in the fluorescence quenching experiment. However, mutating Arg52, Lys82, Arg153, Lys179, and Lys193 led to drastic decreases in association with the lipid spots. The difference in fold change between this assay and the fluorescence quenching assay suggests that these mutations do not have an effect on the protein reorganization or fusiginic activity that is an inherent characteristic of the domain[5] but the mutation only decreases the protein association activity. The combination of the kinetic analyses indicated that Arg52, Arg153, Lys179, and Lys193 might play a significant role in the mechanism that mediates Amot association with membranes.

Table 3. Lipid Binding Affinities for POPC/POPE/soy PI/Chol (2/1/1/1) Vesicles Determined by PLO (n = 3)

mutation	AC50 (μM)	std error	fold change
Y11,47,67,118F	16	2	
R52G	288	2	18
K82E	471	2	30
K87E	55	14	3
R153G	289	2	18
R166G	25	2	2
K179E	212	7	13
K193E	171	2	11
R219E	21	3	1

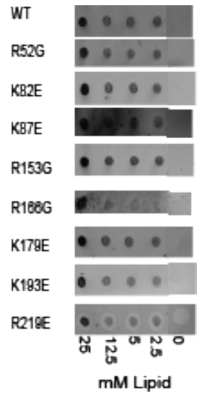

Figure 6. The relative level of protein bound to lipid spots in the PLO assay. The relative level of binding to POPC/POPE/PI/Chol (2/1/1/1 molar ratio) lipid spots adsorbed on to nitrocellulose membranes as a function of lipid concentration as measured by the protein lipid overlay (PLO) assay using fluorescence intensity analysis in LiCOR Odyssey v1.2.

Amot80 Cellular Localization. To further confirm the role of these residues on membrane affinity, the residues were then mutated in full-length Amot80 for the determination of their effect on cellular localization. As previously reported, wild-type Amot80 localizes at the plasma membrane and at cell-to-cell contacts.[1,3,5] In contrast, deletion of the ACCH domain ablated membrane affinity, as evidenced by a complete redistribution of protein to the cytosol.[5] Variants of Amot80 were constructed with the Arg153Glu, Lys179Glu, or Lys193Glu mutation based on our hypothesis that conversion of positively charged residues into negatively charged ones will

DOI: 10.1021/acsomega.9b00165
ACS Omega 2019, 4, 6726−6736

prevent association with negatively charged PI membranes. Mutants were subcloned into a YFP lentiviral construct for stable expression in MCF7 cells (Figure 7). The percentage of cells in which YFP-tagged protein concentrated at cell contacts and puncta was then compared to those having a cytosolic distribution (Figure 8).

Figure 7. Live confocal images of fluorescence in MCF7 cells stably expressing YFP constructs (empty vector, full-length Amot80 wild type, R153E, K179E, and K193E). Scale bars represent 10 μm.

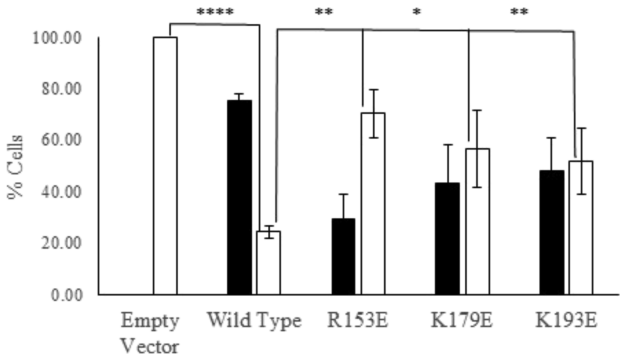

Figure 8. Quantification of the percent of cells with YFP-tagged protein mainly localizing to cell contacts and puncta (black bar) versus intracellular (white bar) expression in relation to the localization of the empty vector and full-length Amot80 (wild type and mutants). Results shown are in biological triplicate, and error bars represent the standard deviation of each sample, p values against the wild-type expression: *** < 0.0005; ** < 0.005 * < 0.05.

Imaging of the R153E, K179E, and K193E mutants revealed an increased distribution to the cytosol versus wild-type Amot80. Because these effects were not as complete as the effects previously observed upon deletion of the ACCH domain, these mutants may still bind to previously described membrane proteins in its signaling pathway. One limitation of this approach is that many of the cells expressing the mutated protein had an increased amount of protein expressing at cytosolic puncta. Therefore, we fractionated the cells to better determine the amount of YFP-tagged Amot protein associated with all membranous bodies (Figure 9). In comparison to the wild-type protein, Amot80 containing a mutation at Arg153, Lys179, and Lys193 led to a decrease in the Amot80 localization in membranous fractions and increased localization in cytosolic fractions. t-tests suggest that there is no significant difference between the amount of mutated Amot associated with the membranes and the cytosol. However, there is a significant difference in the ratio of membranous/cytosolic protein associations between the wild-type and mutant proteins ($p < 0.05$). Furthermore, there is no statistically significant difference between the relative associations of the mutant protein versus the expression of the empty vector ($p > 0.5$). These results suggested that Arg153, Lys179, and Lys193 all play a role in Amot association with membranes.

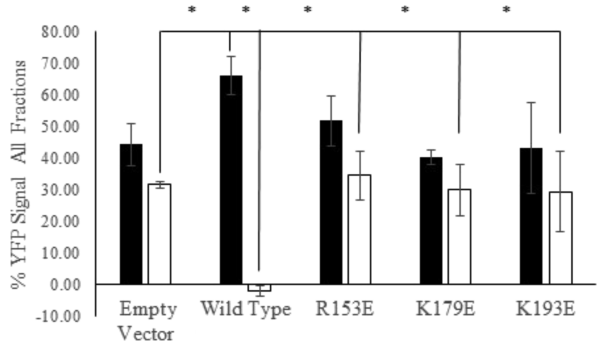

Figure 9. Cellular fractionation of MCF7 cells stably expressing YFP constructs. The relative ratio of membranous (black bar) and cytosolic (white bar) protein as determined by YFP tag fluorescence for the empty vector and full-length Amot80 (wild type and mutants). This assay is unable to resolve intracellular membrane proteins from other lipid environments within the cell. Results shown are in biological triplicate, and error bars represent the standard deviation of each sample. * denotes $p < 0.005$.

DISCUSSION

This study was designed to systematically determine the relative contribution of conserved positively charged residues within the ACCH domain that mediate lipid binding by Angiomotin. To this end, each lysine and arginines in the ACCH domain was mutated into either an acidic or a neutral natural amino acid. Each of these mutants were then subjected to initial screens for their ability to bind lipids, characterization of the effect on native functions and kinetic lipid binding affinity, and determination of effects on Amot80 intracellular localization. Each of the mutants had similar stability and were able to be purified in a similar manner as the wild-type protein, suggesting that most mutations had little effect on overall protein folding. Some of the key residues screened with a glycine mutation were also confirmed using the acidic glutamate mutation later in the study.

Two orthogonal screens were used to identify ACCH domain mutants that had reduced lipid binding. This was done to reduce the impact of limitations in each assay. Fluorescence quenching has long been used to study direct interactions with naturally fluorescent amino acids.[14−16] In this work, the quencher is homogeneously mixed throughout the MLV. Decreased quenching could then be a result of decreased membrane association and/or decreased membrane deformation/re-organization. We have recently reported that PE and PI lipids in this mixture phase-separated from PC lipids, including those containing fluorophores, until the ACCH domain reorganizes them into homogeneous membranes.[9] This would suggest that our fluorescence quenching assay may also show significant changes in fluorescence quenching based on the mutant's ability to reorganize phase separations in the membrane. Therefore, we also incorporated the lipid sedimentation assay as a screen, an assay frequently used to determine the protein's ability to associate with lipids.[5,17,18] This assay would target changes in membrane association without discriminating for membrane reorganization. The requirement of having changes in membrane association from both assays serves to assure that the mutations selected retained their native membrane joining activity,[5] a key function in regulating itself and associated proteins to vesicles that are recycled to the apical plasma membrane, regulating apical/basal polarity and the sequestration of transcription cofactors

DOI: 10.1021/acsomega.9b00165
ACS Omega 2019, 4, 6726−6736

responsible for controlling cellular growth, and migration and proliferation away from the nucleus.[3,10,19,20]

Mutants were also tested for their ability to oligerimerize. Studies have shown Amot heterodimerizes itself, with Amot130 and with AmotL1.[10] Furthermore, the Amot80 dimerization with Amot130 causes it to localize away from actin and into cytosolic vesicles in a similar pattern as an Amot80 homodimer.[10] The amino acid sequence suggests that this domain contains coiled coils, which may mediate this ability to form dimers. Therefore, we chose to eliminate those mutations that lost the ability to form dimers as we have hypothesized that this function is critical to the ability to deform and fuse membranes.[21] The literature is also unclear as to whether the ability to form dimers is critical for membrane association. Hence, our screening assays would not be able to account for the loss of this dimer formation as the driving force for the decreased membrane affinity for membrane or the loss of cellular protein enrichment and localization. As a result, we utilized size exclusion chromatography to eliminate the Arg85 mutations from further study as it only formed monomers.

The lipid binding affinity for the remaining eight mutants was then characterized. Unlike the fluorescence quenching assays, in the PLO assay, the lipid is completely adsorbed to the surface of the nitrocellulose, thereby allowing for more contact with all of the lipids. The combination of the two studies allowed us to accurately determine which mutations had the greatest effect on lipid binding. The fluorescence quenching assay showed the largest decrease in the lipid binding affinity for Arg52, Lys87, and Lys179, while the PLO assay showed similar trends. Mutating Lys87 led to a more significant change in binding for the rest of these mutations except Arg219. The differences in the binding affinities reported can be accounted for by the difference in the presentation of the lipid concentration, as the PLO data was more similar in scale to those previously reported using surface plasmon resonance.[5]

The relative effect of mutating these residues was then considered within the context of the predicted secondary structure of the domain (Figure 10) and our previously

Figure 10. Predicted secondary structure of the ACCH domain using GOR4, where 85.66% is α-helical (underlined), 1.64% is an extended strand, and 12.7% is randomly coiled (italicized).

predicted structure of this domain.[21] The ACCH domain was predicted to be comprised of a coiled coil,[5] where Arg52 and Lys87 are in the middle of the first α helix and Arg153, Lys179, and Lys193 are in the middle of the second α helix (Figure 10). Lys179 and Lys193 may be along the surface of an α helix. However, it was not clear how close in proximity this coil would be in reference to the aforementioned residues, Arg52 or Lys87, or how this secondary coil assists the binding pocket in binding lipids. In addition, all of these residue charges are conserved across all of the Amot family members, further suggesting that they may be important for lipid binding.

Several failed attempts have been made to resolve the atomistic structure of this domain; however, we were able to combine small-angle X-ray scattering and a homology model building technique to create a theoretical model that could be tested by the current results.[21] Our theoretical model suggests that the first α-helical region participates in forming a dimer interface while the second helix may play a stabilizing role in the lipid binding mechanism.[21] Figure 11 contains pictorial

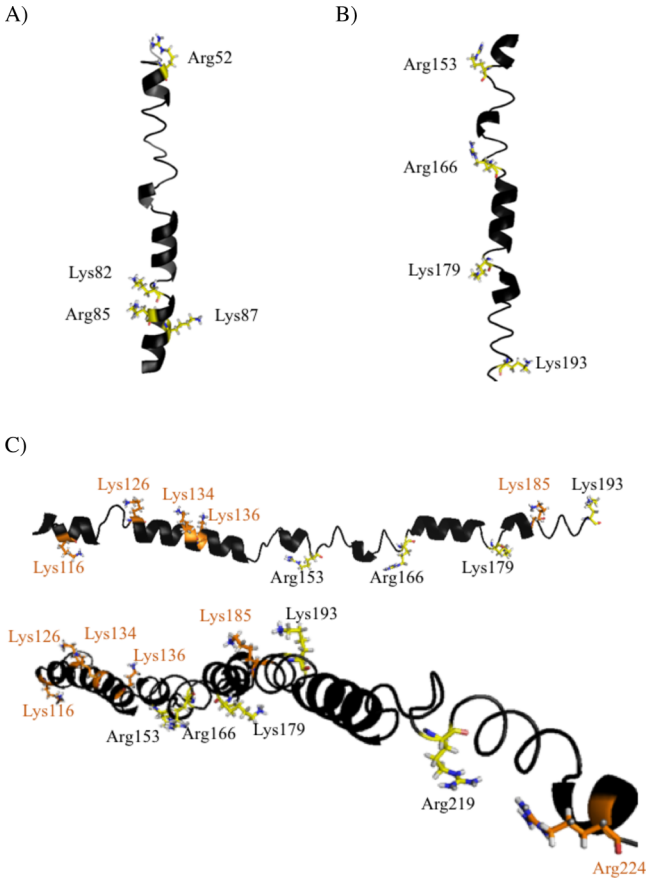

Figure 11. Theoretical structure of the ACCH domain. (A) Dimer interface residues suggested to mediate membrane association. (B, C) Membrane interface residues suggested to mediate membrane association (black) versus the conserved arginine and lysine residues that were not found to have a significant role in membrane association (orange).

representations of this structure while highlighting particular regions of interest based on the current research findings in the proposed dimer and membrane interfaces (Figure 11A,B, respectively). Interestingly, highlighting the residues in the second helical region that were shown in this study to mediate association (black) versus those that did not (orange) suggests that being positioned within a defined helix decreases a mutation's ability to affect membrane association while being positioned within more flexible regions of the domain may be key in mediating charge-related membrane association (Figure 11C).

Arg52, Arg153, and Arg166 were identified as potential targets in preliminary screens where the arginine had been mutated to a glycine. The mutation had no significant effect on purification and stability, thereby suggesting nonsignificant

DOI: 10.1021/acsomega.9b00165
ACS Omega 2019, 4, 6726−6736

effects on protein folding. However, we recognize the usage of glycine as an alternative to the reversal of charge could have a result in localized instability in the α-helical nature of the coiled coil. Other reports suggest that glycine can play a key role in homodimerization of protein α helices, are predominantly oriented toward helix−helix interfaces, and have a high occurrence at helix crossing points.[22,23] Our theortical model's first α-helical region is composed of four main homodimerization interfaces.[21] Arg52 was suggested to fall within the second interface that would be stabilized by a knob-in-hole structure (Figure 11A). Therefore, we suggest that the introduction of this glycine mutation would probably have a little effect. Our theoretical model also suggests that residues 107−236 are located outside of this dimer interface,[21] potentially playing a role in the protein−membrane interface, and that both Arg153 and Arg166 lie within the less rigid random coil structures on the same interface (Figure 11B). This also suggests that introduction of the glycine mutation probably had less of an effect on the local structure of the domain but may be able to play key roles in membrane dynamic associations. Furthermore, we suggest that Arg153, Arg166, Lrys179, and Arg219 all lie along the same membrane association interface while Lys193 may lie along the opposite interface, thereby providing a potential rationale for having flexible regions of the domain. Additionally, other studies have suggested that arginine and lysine residues are not equivalent in their charge, leading to potential critical differences in membrane interactions. Joseph et al. suggests that arginine's guanidinium group could form up to six hydrogen bonds while lysine formed much fewer and more flexible salt bridges.[24] In this protein, we studied seven conserved arginine and four conserved lysine residues in the predicted membrane interface region, resulting in the identification of Arg219 as the only conserved arginine that mediates membrane interactions. The current study used nonphosphorylated PI, which reduced the amount of potential salt bridges that could potentially chemically stabilize the protein−lipid association. Further studies with various levels of PI phosphorylation are needed to further refine the role of forming hydrogen-bond salt bridges as a mechanism for arginine versus lysine mediated membrane association and selectivity.

In polarized epithelial cells, Amot family member cellular localization has major consequences on cellular phenotypes and has been linked to the initiation of various cancers, including renal cell carcinoma,[25] highly invasive and metastatic breast tumors,[3,26,27] osteosarcoma,[28,29] prostate cancer,[30] head and neck squamous cell carcinoma,[31] hepatic carcinoma,[32] ovarian cancer,[33] lung cancer,[34] and gastric adenocarcinomas.[35] As an adaptor protein, Amot80 has been shown to play a significant role in redistributing protein complexes that maintain the morphology and function of intracellular junctions and cell adhesion complexes responsible for planar proliferation associated with normal epithelial stratum.[36] Furthermore, Amot130 cellular localization has been shown to play a significant role in modulating HIPPO-related growth control by redistributing cofactors YAP and TAZ, where membrane association inhibits pro-proliferation transcription programs[37−39] and nonmembrane association causes cell cycle activation.[40,41] Therefore, determining the effect of mutating the residues within the context of the cellular environment was key. The full-length Amot80 cellular localization studies suggested that mutating Lys179 and Lys193 completely disrupted ACCH domain function. However, the cellular fractionation results from the Arg153 mutation suggest that it had less of an effect on lipid association in full-length Amot80 than the other two mutations. As the live cell imaging suggests a greater change in localization, we hypothesized that the protein may still be associated with inositol or negatively charged headgroup containing vesicles within the cell. Therefore, future studies should look at the role of this residue lipid selectivity. Based on the collection of cellular works presented, we confirmed that three residues play a significant role in lipid binding: Arg153, Lys179, and Lys193. Further studies need to confirm the role of Arg52 and Lys87.

Another confirmation of the role of mutating Arg153 comes from patient data reported in the cBioPortal for Cancer Genomics.[42,43] That data suggests that mutating the Arg153 residue in both Amot80 and Amot130 to a histidine has been the linked to the occurrence of a stomach cancer, gastric signet ring cell carcinoma. This correlation suggests that the loss of lipid binding associated with this charged amino acid is linked to the initiation and progression of stomach adenocarcinoma due to the loss of the regulation of the adaptive function of this protein associated with the ability to colocalize with the plasma membrane and other membranous organelles. Specifically, the mutation of arginine to a histidine, a residue with a lower pK_a, would lead to the incorporation and presentation of a mostly deprotonated residue. There have been reports in other proteins such as epidermal growth factor receptor (EGFR) and tumor protein 53 (p53) where the cancer causing Arg mutation in nonprotonated histidine can cause drastic tilting of the residue and α-helical shifts.[44] We would hypothesize that this mutation with the ACCH domain lipid binding would not only eliminate the charge−charge interaction with the inositols of the membrane but may also cause tilting, creating more steric hinderances to the interactions that support protein−lipid interactions in that region of the C terminus. Future studies should utilize various protonation state mutations for Arg153 as a means to study Amot family members and their adaptive role in the signaling pathway responsible for the initiation of oncogenic cellular phenotype.

CONCLUSIONS

In conclusion, this work paves the way for a detailed understanding of the mechanisms involved in ACCH domain lipid binding. We hypothesized that the ACCH domain had a similar mechanism to other phosphatidylinositol binding membranes, where basic residue patches mediate the affinity. This study used a detailed screening of the lysines and arginines to determine their individual roles in mediating this function and found three residues that appear to play a significant role in this membrane affinity while having little to no effect on other native domain functions. Furthermore, we were able to determine that these three residues (Arg153, Lys179, and Lys193), which are predicted to lie along the same face of the α helix providing a positively charged surface to contact the negatively charged membrane,[21] significantly increased cytosolic localization of full-length Amot80. Because mutation of one of these residues is linked to the initiation of stomach cancer, future studies may expand on the results here to determine how mutations in this residue effects, and the resulting loss of Amot membrane association, may influence the appearance of stomach cancerous phenotypes.

DOI: 10.1021/acsomega.9b00165
ACS Omega 2019, 4, 6726−6736

EXPERIMENTAL

Materials. *N*-(5-Dimethylaminonaphthalene-1-sulfonyl)-1,2-dihexadecanoyl-*sn*-glycero-3-phosphoethanolamine (dansyl DHPE) and SYPRO Red Protein Gel Stain was purchased from Invitrogen Life Technologies (Grand Island, NY). 1-Palmitoyl-2-oleoyl-*sn*-glycero-3-phosphocholine (POPC), 1-palmitoyl-2-oleoyl-*sn*-glycero-3-phosphoethanolamine (POPE), soy L-α-phosphatidylinositol (PI), and ovine wool cholesterol (Chol) were purchased from Avanti Polar Lipids (Alabaster, AL). Dodecyl thiomaltopyranoside was purchased from Anatrace (Maumee, OH). All other materials were purchased from Fisher Scientific (Pittsburgh, PA). Unless otherwise noted, the buffer solution used for all experiments contained 50 mM Tris, 600 mM HEPES, 300 mM NaCl, 0.5 mM EDTA, 1 mM DTT, 4 mM benzamidine, and 24.7 μM dodecyl thiomaltopyranoside (elution buffer).

Plasmids. The ACCH domain sequence was previously cloned into the pGEX vector.[1,5,45−47] Mutations in the DNA sequence were cloned into the vector using Pfu polymerase AD in a site-directed mutagenesis polymerase chain reaction. Lentiviral yellow fluorescent protein (YFP) full-length Amot80 constructs from a previous report were used to clone in DNA fragments containing specific mutations (Genewiz) for expression as full-length protein.[3]

Protein Purification. The Amot ACCH domain cDNA was subcloned into the pGEX expression plasmid and transformed into *Escherichia coli* BL21 (DE3) cells.[48] Cells were grown in 2× TY medium with 100 mg/L ampicillin at 37 °C. Isopropyl-β-D-thiogalactopyranoside (0.1 mM) was used to induce protein synthesis at 16 °C overnight. Cells were pelleted by centrifugation, solubilized in lysis buffer (phosphate-buffered saline solution containing 1 mM DTT, 4 mM benzamidine, and 24.7 μM dodecyl thiomaltopyranoside), and lysed using 50 g/L lysozyme,[49] and the lysate was then collected by centrifugation.[50−52] Proteins were purified using batch purification of glutathione resin[53−55] and eluted with an additional 50 mM glutathione. The proteins were analyzed for purity using SDS−PAGE and concentrated using a 10 kDa filter tube to ≥32 μM.

Liposome Preparation. Following previously described methods, MLV liposomes were prepared by hydrating 10−60 mg of lyophilized lipid powder in 1−6 mL buffer solution to make a final lipid concentration of 10 mM.[56,57] To ensure complete mixing, solutions were heated above their melting temperatures to 90 °C for an hour, put through three freeze/thaw cycles, and then sonicated for over an hour on an ice bath. The lipid mixture was equilibrated for more than 3−5 days and stored at 4 °C.

Consensus Sequence Identification. The Weblogo tool (http://weblogo.berkeley.edu/) was used to generate the consensus sequence of Amot80/130, AmotL1, and AmotL2 sequences.[58] Furthermore, the tool was used to generate a pictorial representation of the conservation of our library of mutations at the lysine and arginine residues.

Fluorescence Quenching. We have modified previously reported methods for intrinsic fluorescence quenching by substrates[16,59] to determine quenching of intrinsic tyrosine residues within the ACCH domain as there are no native tryptophan residues. The protein (7 μM) was incubated with liposomes containing 5 mol % dansyl DHPE (tyrosine quencher) at the respective concentrations. Mutation screens were performed against 20 mM lipid (POPC/POPE/PI, 3/1/1 mol fraction). Assays were run using a 384-well black plate (Nunc #264556) and measured using the Molecular Devices Flexstation II 384, where the data was collected using SoftMax Pro v5.3. Biological triplicate measurements were taken based on the tyrosine fluorescence (274 nm excitation/303 nm emission). Changes in tyrosine fluorescence (F) due to each lipid concentration (i) are reported as %Fluorescence using the following equation

$$\%\text{Fluorescence} = F_i/F_0{*}100\% \tag{1}$$

The fluorescence quenching data for a series of lipid concentrations were then fit to the four-parameter sigmoidal equation using SigmaPlot (version 10.0, StatSys) to determine the AC_{50}, the point where 50% of the tyrosine emission was quenched. All data represent the average of three independent experiments.

$$\%F_i = \%F_0 + \frac{100 - \%F_0}{1 + \left(\frac{\text{Conc}_i}{AC_{50}}\right)^{-\text{Hillslope}}} \tag{2}$$

The AC50 was used as a relative measurement for when half of the protein has bound to the liposomes, a general measure of lipid affinity changes. In the mutation analysis, all of the tyrosines, except for Tyr118, were mutated into phenylalanine, allowing one tyrosine to be the fluorescent probe to test for quenching as function of the POPC/POPE/soy PI (3/1/1 molar ratio) multilamellar vesicle concentration.

Sedimentation Assay. We modified the lipid sedimentation assay previously described by Heller et al.[5] to study 20 μM ACCH domain protein affinity for 15 mM lipid with the following modifications. Twenty microliters of ethanol was added to both the lipid pellet and the liquid supernatant sample to solubilize the lipid prior to running a 12% SDS−PAGE gel. Gels were stained using Coomassie blue stain and analyzed using ImageJ version 1.47t. The area and mean were used to calculate the integrated density of each band. Fractions of lipid-bound versus unbound protein were calculated for each mutant and compared against the fraction for the wild type (protein with no mutation) to determine decreases in lipid binding. The percent change in binding between the native protein and the mutant protein of this ratio was then reported.

Characterization of Protein Oligomer State. Purified GST-tagged ACCH domain proteins had their GST tag removed using a previously described methodology using thrombin.[5] Thrombin was removed using 50 kDa centrifugal filters (Millipore). Supernatants were then loaded onto a glutathione resin column, and eluants containing the cleaved protein were collected and concentrated. The purified protein was then loaded onto a Superdex 75 Prep Grade resin (GE Healthcare) column previously equilibrated with the elution buffer and calibrated with low- and high-molecular-weight gel filtration calibration kits (Millipore).

Protein Lipid Overlay (PLO) Assay. The protein lipid overlay (PLO) assay was performed as previously described,[60] with the following procedural modifications. Previously described liposomes were diluted, incubated for 1 h, and then blotted onto the nitrocellulose membrane (Ambersham Hybond ECL Membrane, GE Healthcare). The membrane was then blocked at room temperature for 30 min in PBS buffer containing 0.1% Triton-X and 1% (w/v) nonfat dry milk. The membrane was then incubated for an additional 30 min in 2

DOI: 10.1021/acsomega.9b00165
ACS Omega 2019, 4, 6726−6736

μM purified protein, washed in PBST, and incubated with the anti-GST antibody DyLight 680 conjugate (1/1000 dilution) (MA4-004-D680, Thermo Scientific). The membrane was rinsed in PBST, and the bound protein was then analyzed using a LiCOR Biosciences imaging station where the fluorescence intensity was analyzed using Odyssey v1.2 as previously reported.[3]

Mammalian Cell Culture. Human embryonic kidney (HEK) 293 T cells and MCF7 cells (C. Wells, Indiana University School of Medicine) were cultured in DMEM with 10% FBS at 37 °C in 5% CO2 (v/v). Transfections and lentiviral production were carried out in HEK293T cells, and stable viral infection were carried out in MCF7 cells as previously described.[3,20] Live cell fluorescence images were acquired, and the images were processed and analyzed using Zeiss Axiovision (v. 4.8) using a methodology previously described.[5,20] Cells were also separated into their nuclear, cytosolic, and membranous components (BioVision K270-50) as previously described.[61−65] Aliquots of each fraction (2 μg) were then analyzed for their YFP fluorescence to determine the relative percentage of the YFP-tagged Amot80 found in each fraction.

AUTHOR INFORMATION

Corresponding Author

*E-mail: ankimble@umail.iu.edu.

ORCID

Ann C. Kimble-Hill: 0000-0001-9575-5454

Present Addresses

[#]1433 Jefferson Street, San Francisco, California 94123, United States.

[⊥]2626 Solidago Drive, Plainfield, Indiana 46168, United States.

[∥]212 East 14th Street, New York, New York 10003, United States.

[§]921 Cornell Road, Kokomo, Indiana 46901, United States.

[‡]512 Kennet Ct., Spartanburg, South Carolina 29301, United States.

Author Contributions

The manuscript was written through contributions of all authors. All authors have given approval to the final version of the manuscript. A.K.-H. designed the study, performed the experiments, analyzed the data, and prepared the manuscript. L.H. performed the experiments, analyzed the data, and prepared the manuscript. E.D. performed the experiments. M.A., E.I., I.J.-S., and D.E.J. performed the experiments and analyzed the data. A.F. performed the cloning experiments. C.D.W. provided the initial GST-ACCH domain and YFP Amot80 constructs and performed the cloning experiments.

Funding

This work was supported, in whole or in part, by the National Cancer Institute/National Institutes of Health Grant K01-CA169078.

Notes

The authors declare no competing financial interest.

ACKNOWLEDGMENTS

The authors wish to thank the Indiana University School of Medicine Life Health Science Internship Program, the Indiana University Purdue University Indianapolis Center for Research and Learning Undergraduate Research Opportunity Program and Bridges to Baccalaureate Program, and the American Chemical Society Project Seed program for providing the funding for students to participate in the research. In addition, the authors thank Dr. Quyen Hoang for providing the FlexStation II used for this study. The authors would also like to thank Dr. Thomas D. Hurley for helping in the development of the kinetic fluorescence assay and analysis of the resulting data presented and Dr. Clark D. Wells for providing the initial lentivirus constructs for cloning, expertise in cloning constructs, initial training in mammalian cell culture technique, and equipment for tissue culture.

ABBREVIATIONS

Angiomotin (Amot); Angiomotin coiled-coil homology domain (ACCH); phosphatidylinositol (PI); half maximal active concentration (AC50).

REFERENCES

(1) Wells, C. D.; Fawcett, J. P.; Traweger, A.; Yamanaka, Y.; Goudreault, M.; Elder, K.; Kulkarni, S.; Gish, G.; Virag, C.; Lim, C.; Colwill, K.; Starostine, A.; Metalnikov, P.; Pawson, T. A Rich1/Amot Complex Regulates the Cdc42 GTPase and Apical-Polarity Proteins in Epithelial Cells. *Cell* **2006**, *125*, 535−548.

(2) Vogt, P.; Hart, J. R.; Gymnopoulos, M.; Jiang, H.; Kang, S.; Bader, A. G.; Zhao, L.; Denley, A. Phosphatidylinositol 3-Kinase: The Oncoprotein In *Phosphoinositide 3-kinase in Health and Disease*; Rommel, C., Vanhaesebroeck, B., Vogt, P. K., Eds.; Springer: Berlin Heidelberg, 2011; pp 79−104.

(3) Ranahan, W. P.; Han, Z.; Smith-Kinnaman, W.; Nabinger, S. C.; Heller, B.; Herbert, B.-S.; Chan, R.; Wells, C. D. The Adaptor Protein AMOT Promotes the Proliferation of Mammary Epithelial Cells via the Prolonged Activation of the Extracellular Signal-Regulated Kinases. *Cancer Res.* **2011**, *71*, 2203−2211.

(4) Zhao, B.; Li, L.; Lu, Q.; Wang, L. H.; Liu, C.-Y.; Lei, Q.; Guan, K.-L. Angiomotin is a novel Hippo pathway component that inhibits YAP oncoprotein. *Genes Dev.* **2011**, *25*, 51−63.

(5) Heller, B.; Adu-Gyamfi, E.; Smith-Kinnaman, W.; Babbey, C.; Vora, M.; Xue, Y.; Bittman, R.; Stahelin, R. V.; Wells, C. D. Amot Recognizes a Juxtanuclear Endocytic Recycling Compartment via a Novel Lipid Binding Domain. *J. Biol. Chem.* **2010**, *285*, 12308−12320.

(6) Xu, Y.; Seet, L.-F.; Hanson, B.; Hong, W. The Phox homology (PX) domain, a new player in phosphoinositide signalling. *Biochem. J.* **2001**, *360*, 513−530.

(7) Stenmark, H.; Aasland, R.; Toh, B.-H.; D'Arrigo, A. Endosomal Localization of the Autoantigen EEA1 Is Mediated by a Zinc-binding FYVE Finger. *J. Biol. Chem.* **1996**, *271*, 24048−24054.

(8) Rong, S.-B.; Hu, Y.; Enyedy, I.; Powis, G.; Meuillet, E. J.; Wu, X.; Wang, R.; Wang, S.; Kozikowski, A. P. Molecular Modeling Studies of the Akt PH Domain and Its Interaction with Phosphoinositides. *J. Med. Chem.* **2001**, *44*, 898−908.

(9) Kimble-Hill, A. C.; Petrache, H. I.; Seifert, S.; Firestone, M. A. Reorganization of Ternary Lipid Mixtures of Nonphosphorylated Phosphatidylinositol Interacting with Angiomotin. *J. Phys. Chem. B.* **2018**, 8404.

(10) Ernkvist, M.; Birot, O.; Sinha, I.; Veitonmaki, N.; Nyström, S.; Aase, K.; Holmgren, L. Differential roles of p80- and p130-angiomotin in the switch between migration and stabilization of endothelial cells. *Biochim. Biophys. Acta, Mol. Cell Res.* **2008**, *1783*, 429−437.

(11) Moleirinho, S.; Guerrant, W.; Kissil, J. L. The Angiomotins − From discovery to function. *FEBS Lett.* **2014**, *588*, 2693−2703.

(12) Patrie, K. M. Identification and characterization of a novel tight junction-associated family of proteins that interacts with a WW domain of MAGI-1. *Biochim. Biophys. Acta, Mol. Cell Res.* **2005**, *1745*, 131−144.

(13) Zheng, Y.; Vertuani, S.; Nyström, S.; Audebert, S.; Meijer, I.; Tegnebratt, T.; Borg, J.-P.; Uhlén, P.; Majumdar, A.; Holmgren, L. Angiomotin-Like Protein 1 Controls Endothelial Polarity and

DOI: 10.1021/acsomega.9b00165
ACS Omega 2019, 4, 6726−6736

Junction Stability During Sprouting Angiogenesis. *Circ. Res.* **2009**, *105*, 260−270.
(14) Thomas, L.; Scheidt, H. A.; Bettio, A.; Beck-Sickinger, A. G.; Huster, D.; Zschörnig, O. The interaction of neuropeptide Y with negatively charged and zwitterionic phospholipid membranes. *Eur. Biophys. J.* **2009**, *38*, 663−677.
(15) Poveda, J. A.; Prieto, M.; Encinar, J. A.; González-Ros, J. M.; Mateo, C. R. Intrinsic Tyrosine Fluorescence as a Tool To Study the Interaction of the Shaker B "Ball" Peptide with Anionic Membranes. *Biochemistry* **2003**, *42*, 7124−7132.
(16) Liu, R.; Siemiarczuk, A.; Sharom, F. J. Intrinsic Fluorescence of the P-glycoprotein Multidrug Transporter: Sensitivity of Tryptophan Residues to Binding of Drugs and Nucleotides. *Biochemistry* **2000**, *39*, 14927−14938.
(17) Santonicola, M. G.; Lenhoff, A. M.; Kaler, E. W. Binding of Alkyl Polyglucoside Surfactants to Bacteriorhodopsin and its Relation to Protein Stability. *Biophys. J.* **2008**, *94*, 3647−3658.
(18) Lee, S. A.; Eyeson, R.; Cheever, M. L.; Geng, J.; Verkhusha, V. V.; Burd, C.; Overduin, M.; Kutateladze, T. G. Targeting of the FYVE domain to endosomal membranes is regulated by a histidine switch. *Proc. Natl. Acad. Sci. U. S. A.* **2005**, *102*, 13052−13057.
(19) Bratt, A.; Birot, O.; Sinha, I.; Veitonmäki, N.; Aase, K.; Ernkvist, M.; Holmgren, L. Angiomotin Regulates Endothelial Cell-Cell Junctions and Cell Motility. *J. Biol. Chem.* **2005**, *280*, 34859−34869.
(20) Adler, J. J.; Heller, B. L.; Bringman, L. R.; Ranahan, W. P.; Cocklin, R. R.; Goebl, M. G.; Oh, M.; Lim, H.-S.; Ingham, R. J.; Wells, C. D. Amot130 Adapts Atrophin-1 Interacting Protein 4 to Inhibit Yes-associated Protein Signaling and Cell Growth. *J. Biol. Chem.* **2013**, *288*, 15181−15193.
(21) Peck, C. J.; Virtanen, P.; Johnson, D.; Kimble-Hill, A. Using the predicted structure of the Amot Coiled Coil Homology domain to understand lipid binding. *IUJUR* **2018**, 27.
(22) Brosig, B.; Langosch, D. The dimerization motif of the glycophorin A transmembrane segment in membranes: Importance of glycine residues. *Protein Sci.* **1998**, *7*, 1052−1056.
(23) Javadpour, M. M.; Eilers, M.; Groesbeek, M.; Smith, S. O. Helix Packing in Polytopic Membrane Proteins: Role of Glycine in Transmembrane Helix Association. *Biophys. J.* **1999**, *77*, 1609−1618.
(24) Joseph, P. R. B.; Sawant, K. V.; Iwahara, J.; Garofalo, R. P.; Desai, U. R.; Rajarathnam, K. Lysines and Arginines play non-redundant roles in mediating chemokine-glycosaminoglycan interactions. *Sci. Rep.* **2018**, *8*, 12289.
(25) Lv, M.; Li, S.; Luo, C.; Zhang, X.; Shen, Y.; Sui, Y.; Wang, F.; Wang, X.; Yang, J.; Liu, P.; Yang, J. Angiomotin promotes renal epithelial and carcinoma cell proliferation by retaining the nuclear YAP. *Oncotarget* **2016**, *7*, 12393−12403.
(26) Jiang, W. G.; Watkins, G.; Douglas-Jones, A.; Holmgren, L.; Mansel, R. E. Angiomotin and angiomotin like proteins, their expression and correlation with angiogenesis and clinical outcome in human breast cancer. *BMC Cancer* **2006**, *6*, 16.
(27) Zhang, H.; Fan, Q. MicroRNA-205 inhibits the proliferation and invasion of breast cancer by regulating AMOT expression. *Oncol. Rep.* **2015**, *34*, 2163−2170.
(28) Ruan, W.; Wang, P.; Feng, S.; Xue, Y.; Li, Y. Long non-coding RNA small nucleolar RNA host gene 12 (SNHG12) promotes cell proliferation and migration by upregulating angiomotin gene expression in human osteosarcoma cells. *Tumor Biol.* **2016**, *37*, 4065−4073.
(29) Ruan, W.-D.; Wang, P.; Feng, S.; Xue, Y.; Zhang, B. MicroRNA-497 inhibits cell proliferation, migration, and invasion by targeting AMOT in human osteosarcoma cells. *OncoTargets Ther.* **2016**, *9*, 303−313.
(30) Albrecht, L. V.; Green, K. J.; Dubash, A. D. Cadherins in Cancer In *The Cadherin Superfamily: Key Regulators of Animal Development and Physiology*; Suzuki, S. T., Hirano, S., Eds; Springer Japan: Tokyo, 2016; pp 363−397.
(31) Hakami, F.; Darda, L.; Stafford, P.; Woll, P.; Lambert, D. W.; Hunter, K. D. The roles of HOXD10 in the development and progression of head and neck squamous cell carcinoma (HNSCC). *Br. J. Cancer* **2014**, *111*, 807−816.
(32) Yi, C.; Shen, Z.; Stemmer-Rachamimov, A.; Dawany, N.; Troutman, S.; Showe, L. C.; Liu, Q.; Shimono, A.; Sudol, M.; Holmgren, L.; Stanger, B. Z.; Kissil, J. L. The p130 Isoform of Angiomotin Is Required for Yap-Mediated Hepatic Epithelial Cell Proliferation and Tumorigenesis. *Sci. Signaling* **2013**, *6*, ra77−ra77.
(33) Wang, Y.; Justilien, V.; Brennan, K. I.; Jamieson, L.; Murray, N. R.; Fields, A. P. PKC*ι* regulates nuclear YAP1 localization and ovarian cancer tumorigenesis. *Oncogene* **2017**, *36*, 534−545.
(34) Hsu, Y.-L.; Hung, J.-Y.; Chou, S.-H.; Huang, M.-S.; Tsai, M.-J.; Lin, Y.-S.; Chiang, S.-Y.; Ho, Y.-W.; Wu, C.-Y.; Kuo, P.-L. Angiomotin decreases lung cancer progression by sequestering oncogenic YAP/TAZ and decreasing Cyr61 expression. *Oncogene* **2015**, *34*, 4056−4068.
(35) Ellmark, P.; Ingvarsson, J.; Carlsson, A.; Lundin, B. S.; Wingren, C.; Borrebaeck, C. A. K. Identification of Protein Expression Signatures Associated with Helicobacter pylori Infection and Gastric Adenocarcinoma Using Recombinant Antibody Microarrays. *Mol. Cell. Proteomics* **2006**, *5*, 1638−1646.
(36) Nejsum, L. N.; Nelson, W. J. Epithelial cell surface polarity: the early steps. *Front. Biosci.* **2009**, *14*, 1088−1098.
(37) Zhao, B.; Lei, Q.-Y.; Guan, K.-L. The Hippo−YAP pathway: new connections between regulation of organ size and cancer. *Curr. Opin. Cell Biol.* **2008**, *20*, 638−646.
(38) Mauviel, A.; Nallet-Staub, F.; Varelas, X. Integrating developmental signals: a Hippo in the (path)way. *Oncogene* **2012**, *31*, 1743−1756.
(39) Bao, Y.; Hata, Y.; Ikeda, M.; Withanage, K. Mammalian Hippo pathway: from development to cancer and beyond. *J. Biochem.* **2011**, *149*, 361−379.
(40) Hinck, L.; Näthke, I. Changes in cell and tissue organization in cancer of the breast and colon. *Curr. Opin. Cell Biol.* **2014**, *26*, 87−95.
(41) Shin, K.; Fogg, V. C.; Margolis, B. Tight junctions and cell polarity. *Annu. Rev. Cell Dev. Biol.* **2006**, *22*, 207−235.
(42) Gao, J.; Aksoy, B. A.; Dogrusoz, U.; Dresdner, G.; Gross, B.; Sumer, S. O.; Sun, Y.; Jacobsen, A.; Sinha, R.; Larsson, E.; Cerami, E.; Sander, C.; Schultz, N. Integrative Analysis of Complex Cancer Genomics and Clinical Profiles Using the cBioPortal. *Sci. Signaling* **2013**, *6*, pl1−pl1.
(43) Cerami, E.; Gao, J.; Dogrusoz, U.; Gross, B. E.; Sumer, S. O.; Aksoy, B. A.; Jacobsen, A.; Byrne, C. J.; Heuer, M. L.; Larsson, E.; Antipin, Y.; Reva, B.; Goldberg, A. P.; Sander, C.; Schultz, N. The cBio Cancer Genomics Portal: An Open Platform for Exploring Multidimensional Cancer Genomics Data. *Cancer Discovery* **2012**, *2*, 401−404.
(44) White, K. A.; Ruiz, D. G.; Szpiech, Z. A.; Strauli, N. B.; Hernandez, R. D.; Jacobson, M. P.; Barber, D. L. Cancer-associated arginine-to-histidine mutations confer a gain in pH sensing to mutant proteins. *Sci. Signaling* **2017**, *10*, eaam9931.
(45) Cha, R.; Tilly, W. *PCR primer*; Cold Spring Harbor Laboratory: Cold Spring Harbor, NY, (1995).
(46) Flaman, J.-M.; Frebourg, T.; Moreau, V.; Charbonnier, F.; Martin, C.; Ishioka, C.; Friend, S. H.; Iggo, R. A rapid PCR fidelity assay. *Nucleic Acids Res.* **1994**, *22*, 3259.
(47) Lundberg, K. S.; Shoemaker, D. D.; Adams, M. W. W.; Short, J. M.; Sorge, J. A.; Mathur, E. J. High-fidelity amplification using a thermostable DNA polymerase isolated from Pyrococcus furiosus. *Gene* **1991**, *108*, 1−6.
(48) Colwill, K.; Wells, C. D.; Elder, K.; Goudreault, M.; Hersi, K.; Kulkarni, S.; Hardy, W. R.; Pawson, T.; Morin, G. B. Modification of the Creator recombination system for proteomics applications−improved expression by addition of splice sites. *BMC Biotechnol.* **2006**, *6*, 13.
(49) Shugar, D. The measurement of lysozyme activity and the ultra-violet inactivation of lysozyme. *Biochim. Biophys. Acta* **1952**, *8*, 302−309.
(50) Kimble-Hill, A. C.; Parajuli, B.; Chen, C.-H.; Mochly-Rosen, D.; Hurley, T. D. Development of Selective Inhibitors for Aldehyde

DOI: 10.1021/acsomega.9b00165
ACS Omega 2019, 4, 6726−6736

Dehydrogenases Based on Substituted Indole-2,3-diones. *J. Med. Chem.* **2014**, *57*, 714−722.
(51) Parajuli, B.; Kimble-Hill, A. C.; Khanna, M.; Ivanova, Y.; Meroueh, S.; Hurley, T. D. Discovery of novel regulators of aldehyde dehydrogenase isoenzymes. *Chem.-Biol. Interact.* **2011**, *191*, 153.
(52) Khanna, M.; Chen, C.-H.; Kimble-Hill, A.; Parajuli, B.; Perez-Miller, S.; Baskaran, S.; Kim, J.; Dria, K.; Vasiliou, V.; Mochly-Rosen, D.; Hurley, T. D. Discovery of a Novel Class of Covalent Inhibitor for Aldehyde Dehydrogenases. *J. Biol. Chem.* **2011**, *286*, 43486−43494.
(53) Petrosyan, A.; Ali, M. F.; Verma, S. K.; Cheng, H.; Cheng, P.-W. Non-muscle myosin IIA transports a Golgi glycosyltransferase to the endoplasmic reticulum by binding to its cytoplasmic tail. *Int. J. Biochem. Cell Biol.* **2012**, *44*, 1153−1165.
(54) Ali, M. F.; Chachadi, V. B.; Petrosyan, A.; Cheng, P.-W. Golgi Phosphoprotein 3 Determines Cell Binding Properties under Dynamic Flow by Controlling Golgi Localization of Core 2 N-Acetylglucosaminyltransferase 1. *J. Biol. Chem.* **2012**, *287*, 39564−39577.
(55) Bobba, S.; Ponnaluri, V. K. C.; Mukherji, M.; Gutheil, W. G. Microtiter Plate-Based Assay for Inhibitors of Penicillin-Binding Protein 2a from Methicillin-Resistant Staphylococcus aureus. *Antimicrob. Agents Chemother.* **2011**, *55*, 2783−2787.
(56) Koerner, M. M.; Palacio, L. A.; Wright, J. W.; Schweitzer, K. S.; Ray, B. D.; Petrache, H. I. Electrodynamics of Lipid Membrane Interactions in the Presence of Zwitterionic Buffers. *Biophys. J.* **2011**, *101*, 362−369.
(57) Yamashita, Y.; Oka, M.; Tanaka, T.; Yamazaki, M. A new method for the preparation of giant liposomes in high salt concentrations and growth of protein microcrystals in them. *Biochim. Biophys. Acta, Biomembr.* **2002**, *1561*, 129−134.
(58) Crooks, G. E.; Hon, G.; Chandonia, J.-M.; Brenner, S. E. WebLogo: A Sequence Logo Generator. *Genome Res.* **2004**, *14*, 1188−1190.
(59) Eftink, M. Fluorescence Quenching Reactions. In *Biophysical and Biochemical Aspects of Fluorescence Spectroscopy;* (Dewey, T. G., Ed.), Springer: US, (1991); pp 1−41.
(60) Dowler, S.; Kular, G.; Alessi, D. R. Protein Lipid Overlay Assay. *Sci. Signaling* **2002**, *2002*, pl6−pl6.
(61) Chao, M.-W.; Chen, T.-H.; Huang, H.-L.; Chang, Y.-W.; HuangFu, W.-C.; Lee, Y.-C.; Teng, C.-M.; Pan, S.-L. Lanatoside C, a cardiac glycoside, acts through protein kinase Cδ to cause apoptosis of human hepatocellular carcinoma cells. *Sci. Rep.* **2017**, *7*, 46134.
(62) Ying, Y.; Zhu, H.; Liang, Z.; Ma, X.; Li, S. GLP1 protects cardiomyocytes from palmitate-induced apoptosis via Akt/GSK3b/b-catenin pathway. *J. Mol. Endocrinol.* **2015**, 245−262.
(63) Chen, Y.; Bang, S.; Park, S.; Shi, H.; Kim, S. F. Acyl-CoA Binding Domain Containing 3 Modulates NAD+ Metabolism through Activating Poly(ADP-ribose) Polymerase 1. *Biochem. J.* **2015**, *469*, 189−198.
(64) Cheng, F.; Cappai, R.; Lidfeldt, J.; Belting, M.; Fransson, L.-Å.; Mani, K. Amyloid Precursor Protein (APP)/APP-like Protein 2 (APLP2) Expression Is Required to Initiate Endosome-Nucleus-Autophagosome Trafficking of Glypican-1-derived Heparan Sulfate. *J. Biol. Chem.* **2014**, *289*, 20871−20878.
(65) Pérez, L. M.; Bernal, A.; San Martín, N.; Lorenzo, M.; Fernández-Veledo, S.; Gálvez, B. G. Metabolic rescue of obese adipose-derived Stem cells by Lin28/Let7 pathway. *Diabetes* **2013**, 2368−2379.

DOI: 10.1021/acsomega.9b00165
ACS Omega 2019, 4, 6726−6736